GAS GIANT PROTOPLANET FORMATION: DISK INSTABILITY MODELS WITH DETAILED THERMODYNAMICS AND VARIED ARTIFICIAL VISCOSITY. A. P. Boss, DTM, Carnegie Institution of Washington (boss@dtm.ciw.edu).

Three dimensional (3D) hydrodynamical models of the evolution of marginally gravitationally unstable protoplanetary disks have shown that such disks are likely to form self-gravitating clumps that could become gas giant protoplanets, even when detailed thermodynamics is included [1]. Vertical convective motions appear to be crucial for providing a means of cooling the disk midplane sufficiently for clump formation [2]. Clump survival to form gas giant planets seems possible, provided that the clumps are sufficiently well-resolved [3]. However, calculations where artificial viscosity is employed generally have not found robust clump formation in either fully 3D [4] or thin disk models [5]. The lack of clump formation in the latter models [5] may be due to the prohibition against vertical convection in thin disk models. Here we show that when artificial viscosity is included in 3D disk models with radiative and convective cooling, the tendency to form clumps is reduced somewhat, but not eliminated, unless the artificial viscosity is increased by a factor of ten. This result suggests that disk instability remains as a possible means for forming the giant planets of our Solar System [7].

Artificial viscosity can be used to help stabilize numerical schemes and to provide microphysical heating within shocks. We use a tensor artificial viscosity [8], which enters into the momentum equations as follows, where the other terms on the right hand sides of these equations are suppressed for clarity,

$$\frac{\partial(\rho v_r)}{\partial t} + \nabla\cdot(\rho v_r \vec{v}) = ... - \frac{1}{r^3}\frac{\partial(r^3 Q_r^r)}{\partial r},$$

$$\frac{\partial(\rho v_\theta)}{\partial t} + \nabla\cdot(\rho v_\theta \vec{v}) = ... - \frac{1}{rsin\theta}\frac{\partial(sin\theta Q_\theta^\theta)}{\partial \theta} + \frac{Q_\phi^\phi cot\theta}{r},$$

$$\frac{\partial(\rho A)}{\partial t} + \nabla\cdot(\rho A \vec{v}) = ... - \frac{\partial Q_\phi^\phi}{\partial \phi},$$

where ρ is the mass density, $\vec{v} = (v_r, v_\theta, v_\phi)$ is the velocity, $A = rsin\theta v_\phi$ is the specific angular momentum, and the Q terms are tensor artificial viscosities. The artificial viscosity is set equal to zero when the divergence of the velocity field ($\nabla\cdot\vec{v}$) is positive (i.e., in expanding regions), and when the divergence is negative, is defined to be

$$Q_r^r = l_r^2\ \rho\ \nabla\cdot\vec{v}\,(\frac{\partial v_r}{\partial r} - \frac{1}{3}\nabla\cdot\vec{v}),$$

$$Q_\theta^\theta = l_\theta^2\ \rho\ \nabla\cdot\vec{v}\,(\frac{1}{r}\frac{\partial v_\theta}{\partial \theta} + \frac{v_r}{r} - \frac{1}{3}\nabla\cdot\vec{v}),$$

$$Q_\phi^\phi = l_\phi^2\ \rho\ \nabla\cdot\vec{v}\,(\frac{1}{rsin\theta}\frac{\partial v_\phi}{\partial \phi} + \frac{v_r}{r} + \frac{v_\theta cot\theta}{r} - \frac{1}{3}\nabla\cdot\vec{v}),$$

where $l_r^2 = max(C_r r^2, C_{\Delta r}\Delta r^2)$, $l_\theta^2 = C_\theta(r\Delta\theta)^2$, and $l_\phi^2 = C_\phi(rsin\theta\Delta\phi)^2$. Δr, $\Delta\theta$, and $\Delta\phi$ are the local grid spacings, $C_{\Delta r}$, C_θ, and C_ϕ are free parameters usually set equal to 1, and C_r is a free parameter usually set equal to 10^{-4}. The contribution to the right hand side of the specific internal energy equation is then

$$E_Q = -Q_r^r\varepsilon_r^r - Q_\theta^\theta\varepsilon_\theta^\theta - Q_\phi^\phi\varepsilon_\phi^\phi,$$

where

$$\varepsilon_r^r = \frac{\partial v_r}{\partial r}, \varepsilon_\theta^\theta = \frac{1}{r}\frac{\partial v_\theta}{\partial \theta} + \frac{v_r}{r}, \varepsilon_\phi^\phi = \frac{1}{rsin\theta}\frac{\partial v_\phi}{\partial \phi} + \frac{v_r}{r} + \frac{v_\theta cot\theta}{r}.$$

E_Q is constrained to be positive or zero, reflecting the role of the artificial viscosity as a dissipative mechanism. When artificial viscosity is to be used, the coefficient C_ϕ normally is set equal to zero in order to preserve the local conservation of angular momentum. Only selected terms from the complete tensor have been employed here. Terms involving coupling the r and θ components with the ϕ components have been dropped (i.e., Q_ϕ^r, Q_r^ϕ, Q_ϕ^θ, and Q_θ^ϕ are neglected), in order to conserve angular momentum locally in a consistent manner (see test cases in [6]).

The models presented here have the standard resolution [1,2] of 100 radial grid points distributed uniformly between 4 AU and 20 AU, 256 azimuthal grid points, 22 theta grid points in a hemisphere (effectively over a million grid points), and include terms up to $l, m = 32$ in the spherical harmonic solution for the gravitational potential. The models begin after 322 years of inviscid evolution of a disk with an initial mass of 0.091 $M_\odot$ [1,2], an outer disk temperature of 40 K, and a minimum Toomre $Q = 1.3$.

The four figures show the results for four 3D models which are identical except for their treatment of artificial viscosity. It can be seen that in the models with the standard artificial viscosity (Fig. 2: $C_{\Delta r} = C_\theta = 1$, $C_\phi = 0$, $C_r = 10^{-4}$; Fig. 3: same as Fig. 2 but $C_\phi = 1$), clump formation occurs in a similar manner as in the model without artificial viscosity (Fig. 1, as in [1,2]). However, when the artificial viscosity is increased by a factor of 10 (Fig. 4), clump formation is significantly inhibited because of the heating associated with the assumed dissipation. These models support the suggestion that microphysical shock heating can be important for clump formation [4], though with the standard amount of artificial viscosity, the effects are relatively minor in these models.

References: [1] Boss, A. P. (2001), *Ap. J.*, **563**, 367. [2] Boss, A. P. (2002), *Ap. J.*, **576**, 462. [3] Mayer, L., et al. (2002), *Science*, **298**, 1756. [4] Pickett, B. K., et al. (2000), *Ap. J.*, **529**, 1034. [5] Nelson, A. F. (2000), *Ap. J.*, **537**, L65. [6] Boss, A. P., & Myhill, E. A. (1992), *Ap. J. S.*, **83**, 311. [7] Boss, A. P., Wetherill, G. W., & Haghighipour, N. (2002), *Icarus*, **156**, 291. [8] Tscharnuter, W. M., & Winkler, K.-H. (1979), *Comput. Phys. Comm.*, **18**, 171.

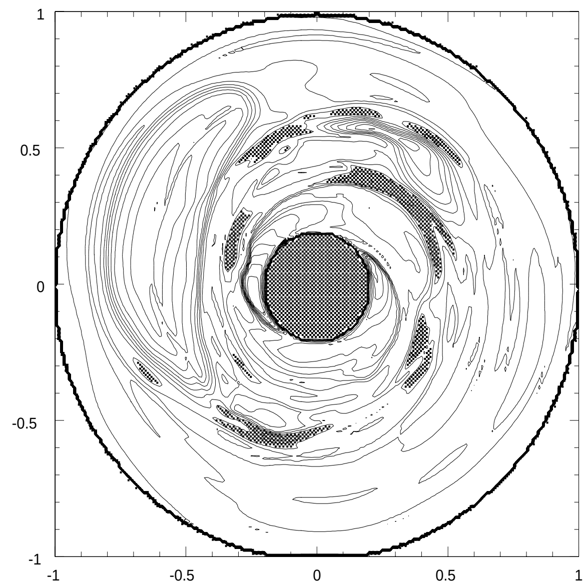

Fig. 1. Equatorial density contours after 366 yrs for the standard model with no artificial viscosity. Hatched regions denote densities above 10^{-10} g cm^{-3}. Contours denote changes by factors of 2. Disk radius is 20 AU.

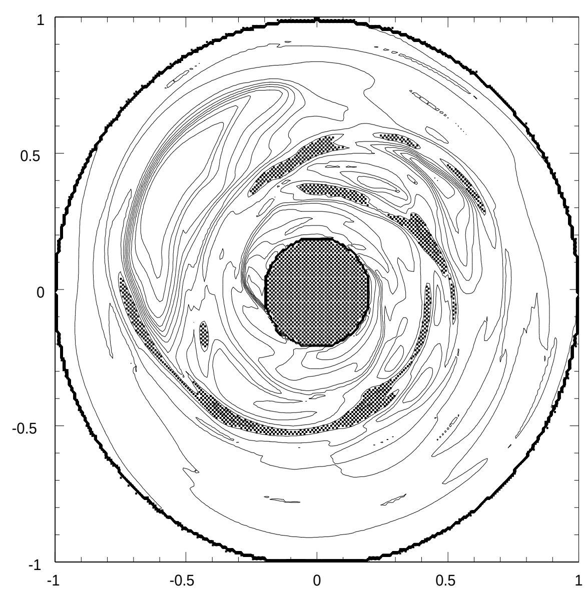

Fig. 2. Equatorial density contours after 364 yrs for model identical to Fig. 1 but with the standard amount of artificial viscosity in r and θ directions only. Clumps still form.

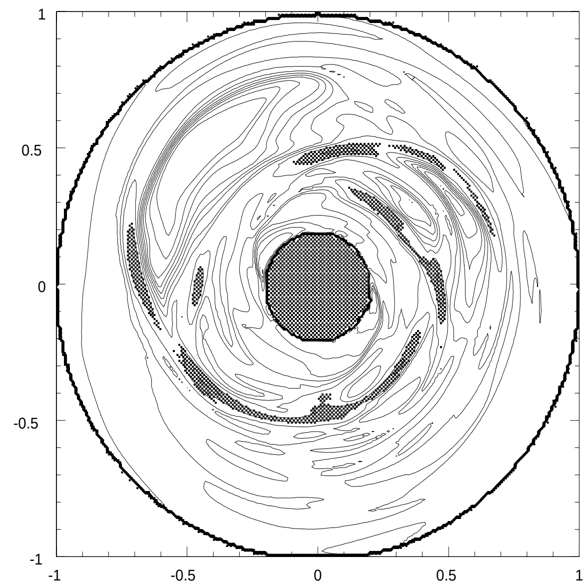

Fig. 3. Equatorial density contours after 362 yrs for model identical to Fig. 1 but with the standard amount of artificial viscosity in r, θ, and ϕ. Clumps still form.

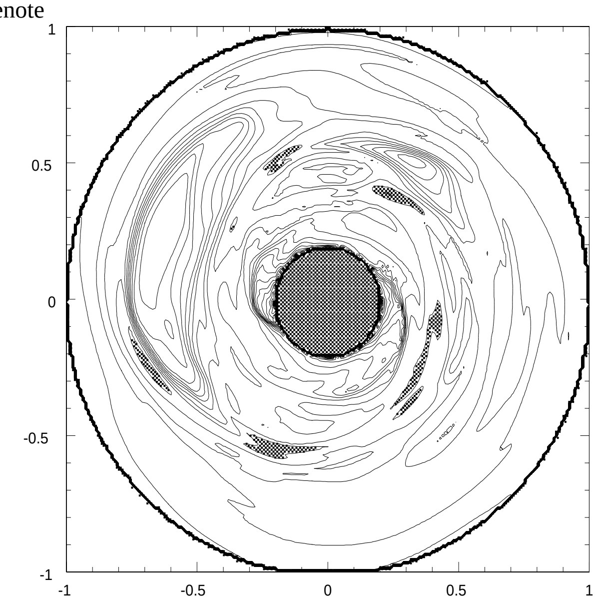

Fig. 4. Equatorial density contours after 366 yrs for model identical to Fig. 1 but with 10 times the standard artificial viscosity in r and θ only. Clump formation is noticeably suppressed.